Deletion of Fas (CD95) in adipocytes relieves adipose tissue inflammation and hepatic manifestations of obesity

Stephan Wueest[1,2], Reto A. Rapold[1,2], Desiree M. Schumann[3], Julia M. Rytka[1,2], Anita Schildknecht[4,5], Alexander V. Chervonsky[6], Assaf Rudich[7], Eugen J. Schoenle[1], Marc Y. Donath[2,3], Daniel Konrad[1,2]

[1]Division of Pediatric Endocrinology and Diabetology, University Children's Hospital, CH-8032 Zurich, Switzerland

[2]Zurich Center for Integrative Human Physiology, University of Zurich, CH-8057 Zurich, Switzerland

[3]Clinic of Endocrinology and Diabetes, [4]Institute of Experimental Immunology, University Hospital Zurich, CH-8091 Zurich, Switzerland

[5]Present address: The Campbell Family Institute for Breast Cancer Research, Ontario Cancer Institute and Department of Medical Biophysics and Immunology, University of Toronto, Toronto, Ontario M5G 2C1, Canada

[6]Department of Pathology, University of Chicago, Chicago, IL 60637, USA

[7]Department of Clinical Biochemistry and the S. Daniel Centre for Health and Nutrition, Ben-Gurion University, Beer-Sheva, Israel

Correspondence to:

Daniel Konrad, M.D. Ph.D.

University Children's Hospital

Department of Endocrinology and Diabetology

Steinwiesstrasse 75

CH-8032 Zurich

Tel: ++41-44-266 7966; Fax: ++41-44-266 7983

Email: daniel.konrad@kispi.uzh.ch

Abstract

Adipose tissue inflammation is linked to the pathogenesis of insulin resistance. Although the death receptor Fas (CD95) activates inflammatory pathways in several tissues, little is known about the metabolic consequence of Fas activation in adipose tissue. The aim of this study was to investigate the contribution of adipocyte-expressed Fas to obesity-associated metabolic dysregulation. Fas expression was significantly increased in adipocytes of insulin-resistant mice and in adipose tissue of obese and obese type 2 diabetic patients. Total body Fas-deficient and adipocyte-specific Fas-knockout (AFasKO) mice were protected from deterioration of glucose homeostasis induced by high fat diet (HFD). Adipocytes of AFasKO mice were more insulin sensitive while mRNA levels of pro-inflammatory factors were reduced in white adipose tissue. Moreover, AFasKO mice did not develop hepatic steatosis and maintained hepatic insulin sensitivity as assessed by clamp-studies. Thus, Fas activation in adipocytes contributes to obesity-associated adipose tissue inflammation, hepatic steatosis and insulin resistance.

Material and Methods

Human Samples

Fat biopsies were taken from women undergoing elective laparoscopic abdominal surgery at the Soroka University Medical Center in Beer-Sheva (Israel) as described and characterized elsewhere (*1, 2*). Patients gave written informed consent to all procedures.

Animals

C57BL/6J wild-type and total body Fas-deficient (Fas-def) mice backcrossed for >10 generations onto this same C57BL/6J inbred strain background (B6.MRL^{lpr}) were obtained from The Jackson Laboratory (Bar Harbor, Maine). Mice with Exon IX of Fas flanked with LoxP sites were produced as described (*3*). Animals with Cre recombinase controlled by the Fabp4-promoter (B6.Cg-Tg(Fabp4-cre)1Rev/J) were purchased from The Jackson Laboratory. All mice were genotyped by PCR with primers amplifying the Cre transgene and Fas generating 319 bp wild-type and 399 bp "floxed" allele products. C57BL/6J wild-type (C57BL/6JOlaHsd)-, ob/ob (C57BL/6OlaHsd-Lep<ob>)- and db/db (BKS.Cg-+Leprdb/+Leprdb/OlaHsd)-mice were purchased from Harlan (AD Horst, The Netherlands).

All mice were housed in a specific pathogen-free environment on a 12-hour light-dark cycle and fed ad libitum with regular chow diet (Provimi Kliba, Kaiseraugst, Switzerland) or HFD (58 kcal% fat w/sucrose Surwit Diet, D12331, Research Diets, New Brunswick, New Jersey). All protocols conformed to the Swiss animal protection laws and were approved by the Cantonal Veterinary Office in Zurich, Switzerland.

Harvesting of naïve splenic macrophages

Splenocytes were isolated in PBS by smashing the spleen through a metal grid with a syringe plunger. After removal of residual tissue, cells were washed and resuspended in 0.4ml MACS buffer (1x PBS, 2% FCS, 5mM EDTA). 20µl of appropriate beads (anti-CD11b, Miltenyi Biotec, Bergisch Gladbach, Germany) were added and the suspension was incubated on ice for 15 minutes. Upon washing, cells were applied to the MACS magnetic separator according to the manufacturer's protocol. To elute the appropriate cells, MACS buffer was pushed through the column with a plunger. For FACS analysis (before

and after MACS), about $3x10^6$ splenocytes were resuspended in FACS buffer (1x PBS, 2% FCS, 0.2% sodium azide, 0.02M EDTA) and stained with anti-CD11b-PE (PharMingen, Becton Dickinson, San Jose, California) labeled antibody. After washing of the cells with FACS buffer, cells were analyzed immediately using FlowJo software (Tree Star, Ashland, Oregon).

Induction of activated peritoneal macrophages by thioglycollate

Three months before use 30g thioglycollate medium (Difco, Chemie Brunschwig AG, Basel, Switzerland) were rehydrated in 1 liter H_20 and autoclaved. For induction of activated peritoneal macrophages, mice were injected i.p. with 1ml thioglycollate suspension. 72 hours later the mice were sacrificed and the peritoneum was flushed with cold PBS in order to harvest the macrophages.

Intra-peritoneal glucose, insulin and pyruvate tolerance tests

For the intraperitoneal glucose tolerance test (ipGTT) mice were fasted overnight, for the intraperitoneal insulin and pyruvate tolerance tests (ipITT, ipPTT) mice were fasted for 3h. Either glucose (2g/kg body weight), human recombinant insulin (0.75U/kg or 1U/kg body weight) or pyruvate (2g/kg body weight) were injected intraperitoneally (*4*).

Glucose incorporation into isolated white adipocytes

Adipocyte isolation was performed as described previously (*5, 6*). To determine glucose incorporation, adipocytes were incubated with D-[U-^{14}C]-glucose (final glucose concentration 0.89mmol/l) for 60 min in the presence or absence of 100nM insulin. Glucose incorporation was stopped by separating cells from the medium by centrifugation through phthalic acid dinonyl ester and then subjected to liquid scintillation counting.

Determination of plasma insulin, adipokines, and free fatty acid levels

Plasma insulin and free fatty acid levels were determined as described (*4*). Plasma adipokine and cytokine levels were determined with mouse LINCOplex kits from Linco Research, Inc. (Labodia, Yens, Switzerland).

Total liver lipid extraction

Liver tissue (30mg) was homogenized in PBS and lipids were extracted in a chloroform-methanol (2:1) mixture. Total liver lipids were determined by a sulfophosphovanillin reaction as previously described (*7*).

RNA extraction and quantitative reverse transcription-PCR (RT-PCR)

Total RNA from fat pads and livers was extracted with the RNeasy lipid tissue mini kit (Qiagen, Basel, Switzerland) and analyzed with a bioanalyzer (Agilent Technologies, Santa Clara, California). 0.75µg of RNA was reverse transcribed with Superscript III Reverse Transcriptase (Invitrogen, Basel, Switzerland) using random hexamer primer (Invitrogen). Taqman system (Applied Biosystems, Rotkreuz, Switzerland) was used for real-time PCR amplification. Relative gene expression was obtained after normalization to 18sRNA (Applied Biosystems), using the formula $2^{-\Delta\Delta cp}$ (*8*). The following primers were used: TNF-α Mm00443258_m1, IL-6 Mm00446190_m1, KC Mm00433859_m1, IL-1β Mm0043422/8_m1, FasL Mm00438864_m1, cd11b Mm00434455_m1, MCP-1 Mm00441242_m1, resistin Mm00445641_m1, SOCS3 Mm00545913_s1, CD36 Mm00432403_m1, ArgI Mm00475988_m1, IL-10 Mm00439614_m1 (Applied Biosystems, Rotkreuz, Switzerland).

Glucose clamp studies

After 5-h fast, hyperinsulinemic-euglycemic clamp was performed in freely moving mice as follows. 3-[^{3}H]glucose was infused for 80 min. After basal sampling, insulin (18mU/kg x min) was infused for 90min. Euglycemia was maintained by a variable infusion of 20% glucose. Insulin-stimulated whole-body glucose metabolism was estimated using 3-[^{3}H]glucose infusion during clamps.

Western Blot

Cell lysates and tissue samples were homogenized in a buffer containing 150 mM NaCl, 50mM Tris-HCl (pH 7.5), 1mM EGTA, 1% NP-40, 0.25% sodium deoxycholate, 1mM sodium vanadate, 1mM NaF, 10mM sodium β-glycerophosphate, 100nM okadaic acid, 0.2mM PMSF and a 1:1000 dilution protease inhibitor cocktail (Sigma). For isolation of total membranes, 3T3-L1 adipocytes were lysed and homogenized in a buffer containing 20mM HEPES, 250mM sucrose, 5mM NaN_3, 1mM EDTA, 0.2mM

PMSF and a 1:1000 dilution protease inhibitor cocktail. Lysates were centrifuged at 50'000 rpm for 90min at 4°C, and pellet was resuspended in homogenization buffer.

Protein concentration was determined using BCA assay (Pierce, Rockford, Illinois) and equivalent amounts of protein (20-50µg) were resolved by LDS-PAGE (4-12% gel; NuPAGE, Invitrogen). Proteins were transferred to a nitrocellulose membrane (0.2µm, BioRad, Reinach, Switzerland) and blocked for one hour in 5% non fat dry milk (BioRad) resolved in Tris buffered saline, containing 1% Tween 20. Membranes were incubated over night at 4°C on a rocking platform with respective primary antibodies. The following primary antibodies were used: anti-GLUT4 (gift of A. Klip, The Hospital for Sick Children, Toronto, Canada), anti-Fas, anti-phospho-IRS1 (Ser307) (Upstate, Lake Placid, New York), anti-Fas (human), anti-IRS-1, anti-PPARγ, anti-C/EBPα and anti-C/EBPβ (Santa Cruz Biotechnology, Santa Cruz, California), anti-ADRP (Novus Biologicals, Littleton, Colorado), anti-Cre and anti-actin (Millipore, Zug, Switzerland), anti-phospho-NF-κB p65 (Cell Signalling, Beverly, MA, USA). Subsequently, membranes were incubated with secondary antibody (horseradish peroxidase-conjugated; Santa Cruz Biotechnology, and Alexis Biochemicals, Lausen, Switzerland) for 1 hour at room temperature. Bands were detected after 5 minute incubation with Lumi-Light substrate (Roche). Membranes were exposed in an Image Reader and analyzed with Image Analyzer (FujiFilm, Dielsdorf, Switzerland).

Determination of 2-deoxy-^{3}H-D-glucose (^{3}H-2dG) uptake and lipolysis in 3T3-L1 cells

3T3-L1 cells were grown and differentiated into adipocytes as described (*5*). ^{3}H-2dG-uptake and lipolysis was measured in mature 3T3-L1 adipocytes as previously reported (*5, 9*).

Macrophage adherence assay

Thioglycollate-activated macrophages (as described above) were labeled with ^{3}H-2dG (*10*) by incubation with HEPES buffer saline containing 2.5mM D-glucose and 5µCi/ml ^{3}H-2dG for 1 h at 37°C. Glucose uptake was stopped by two washes with cold HEPES buffer saline. Labeled macrophages were resuspended in HEPES buffer saline and added to mature 3T3-L1 adipocytes, treated with or without 2ng/ml FasL for 12h in advance. After one hour of incubation at 37°C, cells were washed and lysed (0.05N NaOH). Finally, radioactivity of lysates was determined by a β-counter.

Data analysis

Data are presented as means +/- SE and were analyzed by Student's *t* test, one sample *t* test or by analysis of variance with a Tukey correction for multiple group comparisons.

Results and Discussion

In obesity, excess adipose tissue accumulation is accompanied by local inflammation, characterized by infiltration of inflammatory cells (*1*) and by elevated production of pro-inflammatory cytokines, jointly activating inflammatory pathways in adipocytes. It is proposed, that the consequential alteration in the composition of secreted products from adipocytes contributes to both local and systemic insulin resistance (*2, 3*). Particularly, liver insulin sensitivity can be impaired by obesity-induced alterations in adipokine secretion and by elevation in fat tissue-derived cytokines and fatty acids (*4, 5*). Fas (CD95), a member of the tumor necrosis factor (TNF) receptor family, plays an important role in the regulation of programmed cell death (apoptosis). Fas ligand (FasL) binding to Fas assembles the death inducing signaling complex (DISC), which in turn leads to apoptosis via the activation of caspase 8 and caspase 3. However, like TNFα, Fas activation can also induce non-apoptotic signaling pathways (*6*). For example, Fas activation was shown to induce secretion of pro-inflammatory cytokines like IL-1α, IL-1β, IL-6, IL-8 (KC) and MCP-1 in different cell lines and tissues (*7-11*), rendering it a potential key component in the inflammatory response. Although Fas was shown to be expressed in pre-adipocytes and adipocytes (*12*), little is known about non-apoptotic consequences of Fas activation in adipocytes, and particularly, its role in adipose tissue inflammation and in the dysregulation of metabolism that accompanies obesity.

As an initial step in assessing the possibility that adipocyte Fas is involved in obesity-related fat and whole-body insulin responsiveness, we determined its expression in isolated adipocytes from insulin-resistant mice. Adipocytes were isolated from perigonadal fat pads of 3-months-old ob/ob and db/db mice and their wild-type (WT) controls. Fas protein-expression was determined and normalized to β-actin expression, a commonly-used house keeping gene in adipocytes and adipose tissue (*13*) (fig. 1A). Fas protein levels were significantly increased in ob/ob as well as db/db mice compared to their wild-type controls. Similarly, Fas protein-expression was increased in adipocytes isolated from perigonadal fat pads of high fat-fed C57Bl6/J mice compared to chow-fed controls (fig. 1B). Finally, we determined Fas expression in human adipose tissue of lean, obese, and obese type 2 diabetic patients. None of the examined patients was treated with any medications that might affect inflammatory pathways in adipose tissue or modulate insulin sensitivity (further basic clinical characteristics of the patients are provided in table S1). Fas expression was increased in fat tissue of obese (body mass index >30 kg/m^2) compared to lean persons. Interestingly, Fas was further elevated in obese patients with a more severe metabolic

compromise manifesting as type 2 diabetes (fig. 1C). Collectively, these data demonstrate that Fas expression is upregulated in isolated adipocytes of common genetic and nutritional mouse models of obesity and insulin resistance, and in adipose tissue of obese and obese-diabetic humans.

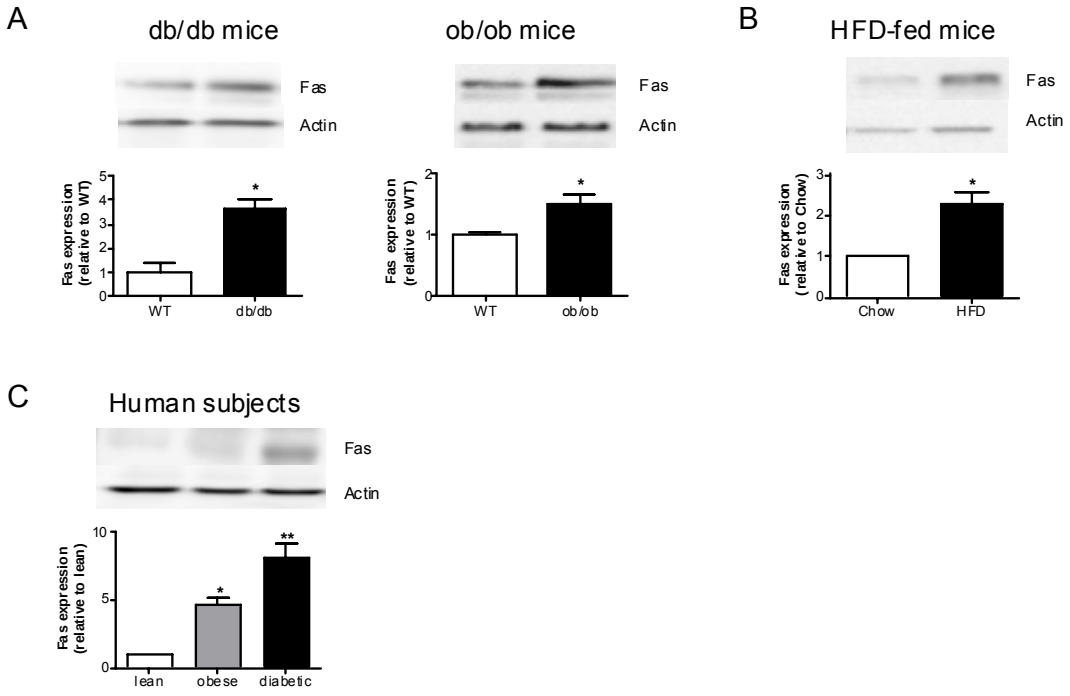

Fig. 1 **(A)** Total cell lysates were prepared from isolated perigonadal adipocytes harvested from db/db, ob/ob and their respective wildtype mice. Lysates were resolved by LDS-PAGE and immunoblotted with anti-Fas or anti-actin antibody. Representative immunoblots are shown. Results are the means ± SEM of 3 mice per group and are normalized to actin expression. *$p < 0.05$ (Student's *t* test). **(B)** Total cell lysates were prepared from isolated adipocytes of perigonadal fat pads of chow-fed and high fat-fed (8 weeks of HFD) C57Bl6/J mice. Lysates were resolved by LDS-PAGE and immunoblotted with anti-Fas or anti-actin antibody. Representative immunoblots are shown. Results are the means ± SEM of 3 mice per group and are normalized to actin expression. *$p < 0.05$ (One sample *t* test). **(C)** Cell lysates from subcutaneous fat biopsies from lean, obese and diabetic patients were prepared and immunoblotted with anti-Fas or anti-actin antibody. Representative immunoblots are shown. Results are the means ± SEM of 3 patients per group and are normalized to actin expression. *$p < 0.05$, **$p < 0.01$ (ANOVA).

To start assessing a putative metabolic role for increased adipocyte Fas expression under insulin-resistant conditions, we analyzed glucose tolerance in total body Fas-deficient (Fas-def) mice (*14*). Fas-def or wild-type mice were fed regular chow or high fat diet (HFD) for six weeks. The latter condition was sufficient to induce a significantly impaired glucose tolerance in wild type mice, though the degree of impairment was less than reported following a longer duration of high fat feeding (20 weeks), hence reflecting early metabolic adaptation to this diet. Total body weight gain was similar in Fas-def and wildtype mice (fig. S1A). However, perigonadal fat pad weight was significantly lower in HFD-fed Fas-def mice compared to WT mice (fig. S1B), and adipocyte size distribution was shifted to the left, reflecting smaller mean adipocyte size in Fas-def mice (fig. S1C). Our finding of reduced fat pad weight and lack of an increase in adipocyte size under HFD in Fas-def mice may hint towards a role of Fas in modulating adipocyte development and/or differentiation. Consistent with such notion, activation of Fas using FasL during adipogenesis of 3T3-L1 pre-adipocytes reduced markers of differentiation like C/EBPbeta, C/EBPalpha and PPARγ (fig. S2). Thus, Fas may interfere with adipose tissue development and expansion in response to high fat feeding by a combined inhibitory effect on pre-adipocyte differentiation and on the accumulation of hypertrophied adipocytes. Remarkably, these effects in the Fas-def mice were associated with protection against HFD-induced glucose intolerance (fig. 2A). Further consistent with Fas involvement in the induction of whole-body insulin resistance, fasting insulin levels were significantly higher in HFD-fed wild-type mice (fig. 2B). Concurrently, adipocytes isolated from HFD-fed wild-type mice exhibited a marked reduction in insulin-stimulated glucose incorporation compared to adipocytes from Fas-def mice (fig. 2C).

Although the effect of total-body deletion of Fas was supportive for a direct role of adipocyte-expressed Fas in the metabolic-endocrine dysregulation occurring in obesity, Fas deletion also affected adipose tissue adaptation to high fat feeding, potentially affecting metabolism secondary to primary effects on adipose tissue development. To further verify that Fas activation, even as an isolated factor, could directly modulate insulin sensitivity in adipocytes, we utilized 3T3-L1 adipocytes. Cells were stimulated with 2 ng/ml membrane-bound Fas-ligand (FasL) for 12 hours. Such treatment had no negative effect on cell viability and did not increase apoptosis rate as assessed by MTT (fig. S3) and TUNEL-assays (data not shown), respectively. Yet, Fas-activation significantly reduced insulin-stimulated glucose uptake (fig.

2D) and stimulated lipolysis (fig. 2E). These findings support the proposition that adipocyte Fas may directly regulate fat cell metabolism by mechanisms unrelated to Fas-induced cell death.

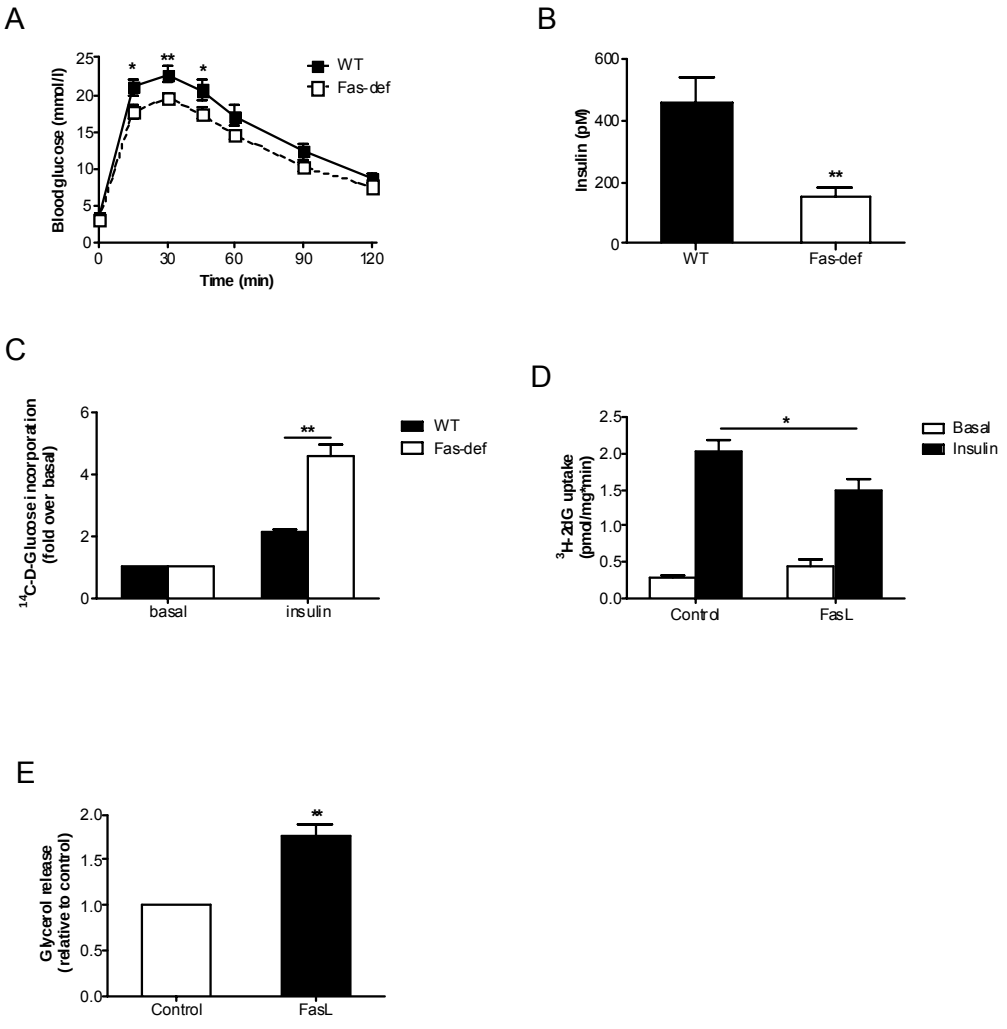

Fig. 2 **(A)** Intraperitoneal glucose tolerance tests in HFD-fed wild-type (■) and Fas-def mice (□). Results are the means ± SEM of 12 to 18 animals per group. *p < 0.05, **p = 0.01 (Student's *t* test). **(B)** Fasting insulin levels were determined in wild-type and Fas-def mice after 8 hours of food withdrawal. Results are the means ± SEM of 4 to 5 animals per group. **p < 0.01 (Student's *t* test). **(C)** ^{14}C-D-glucose incorporation into isolated adipocytes from HFD-fed WT and Fas-def mice was determined in the absence or presence of insulin. Results represent the mean ± SEM of 6 experiments. **p < 0.01 (Student's *t* test). **(D&E)** Mature 3T3-L1 adipocytes were incubated with 2ng/ml FasL for 12 hours. **(D)** 2-deoxy-^{3}H-D-glucose (^{3}H-2dG) glucose uptake was determined after

treatment with or without insulin. Shown are absolute values of ^{3}H-2dG uptake in untreated or FasL-treated 3T3-L1 adipocytes. Results are the mean ± SEM of 9 independent experiments. * $p < 0.05$ (ANOVA). **(E)** Glycerol release was determined after medium was removed and cells were incubated with KREBS buffer for another hour. Results represent the mean ± SEM of 4 independent experiments. **$p < 0.01$ (One sample *t* test).

To test the specific role of Fas expression in adipocytes in the development of insulin resistance in response to HFD-feeding, we generated an adipocyte-specific Fas-knockout mouse (AFasKO) using the Cre-lox system (Fas $^{f/f}$; Fabp4-Cre$^{+/-}$). As a control, floxed Fas mice that do not express Cre-recombinase (Cre) were used (Fas $^{f/f}$; Fabp4-Cre$^{-/-}$). As expected, Fas expression was greatly diminished in isolated white adipocytes of AFasKO mice (fig. 3A), decreased in white and brown adipose tissue, which also includes non-adipocyte cell types (fig. 3B), but was not decreased in other tissue (fig. S4). To gain further insight on the cell type affected by our approach to delete Fas in adipocytes, we next studied macrophage Fas expression, as it was previously claimed that fatty acid binding protein 4 (Fabp4)/aP2 expression was induced in activated macrophages (*15*). Given the fact that cre expression in our mice is under the regulation of the Fabp4 promoter, Fas expression might have been decreased in activated macrophages in addition to adipocytes, thereby influencing adipose tissue biology. However, cre was expressed in adipocytes of AFasKO mice, whereas it was undetectable in macrophages (fig. 3C), consistent with previous studies using the same Fabp4-Cre strain (*13, 16*). Moreover, in both resident (naive) macrophages isolated from the spleen and in activated peritoneal macrophages harvested after thioglycollate injection, Fas protein-expression was not decreased in AFasKO mice (fig. 3D). Collectively, although it still remains possible that a small subpopulation of activated macrophages within adipose tissue express decreased levels of Fas in the AFasKO mice, this novel mouse model exhibits greatly diminished Fas expression in adipocytes but not in other tissues and cell types, including resident and activated peritoneal macrophages. Moreover, since previous studies using the same Fabp4-cre mouse line found no effect of the Cre allele in the first 6 months of life (*16*), AFasKO mice seemed as a useful model to study the in-vivo role of adipocyte Fas expression.

To investigate the functional significance of adipocyte-specific Fas-deletion, AFasKO mice were fed normal chow or HFD for up to 6 weeks. Total body weight gain was similar in AFasKO and their Cre-negative littermates under chow (data not shown) and HFD (fig. S5). After 6 weeks of HFD, inguinal,

perigonadal and retroperitoneal fat pad weights in the AFasKO mice were comparable to WT, whereas mesenteric fat pad weight was slightly, but significantly lower in AFasKO mice (fig. S6). Yet, in contrast to the Fas-def mouse model (fig. S1C), adipocyte size was similar in HFD-fed control or AFasKO mice (fig. 3E). Since Fabp4 is downstream of PPARγ, Cre is only expressed during late stages of adipocyte differentiation in the AFasKO mice (*16*). Thus, early adipocyte-development was likely not affected in AFasKO mice, as opposed to Fas-def mice, and the hypertrophic response of adipocyte to HFD remained similar to control mice.

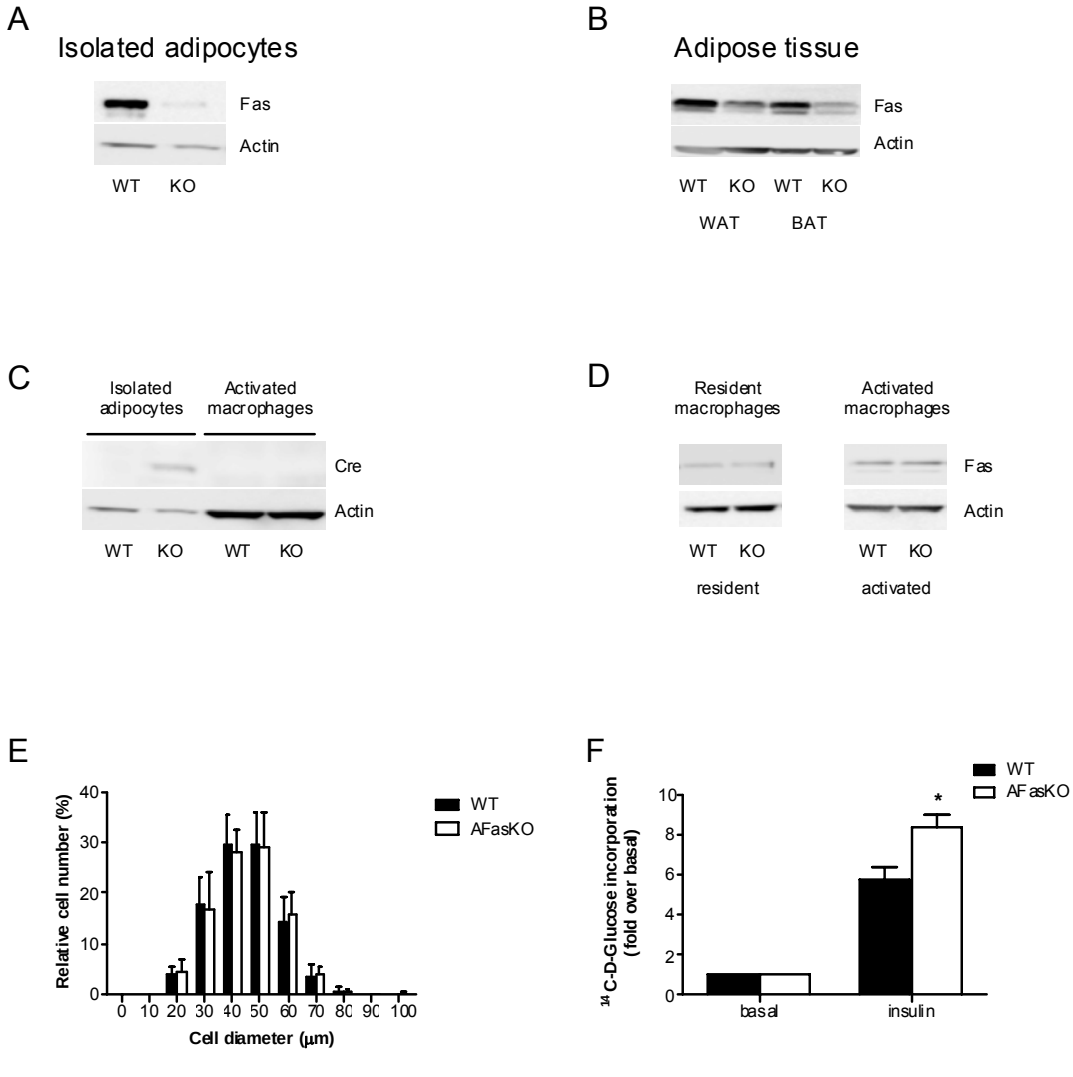

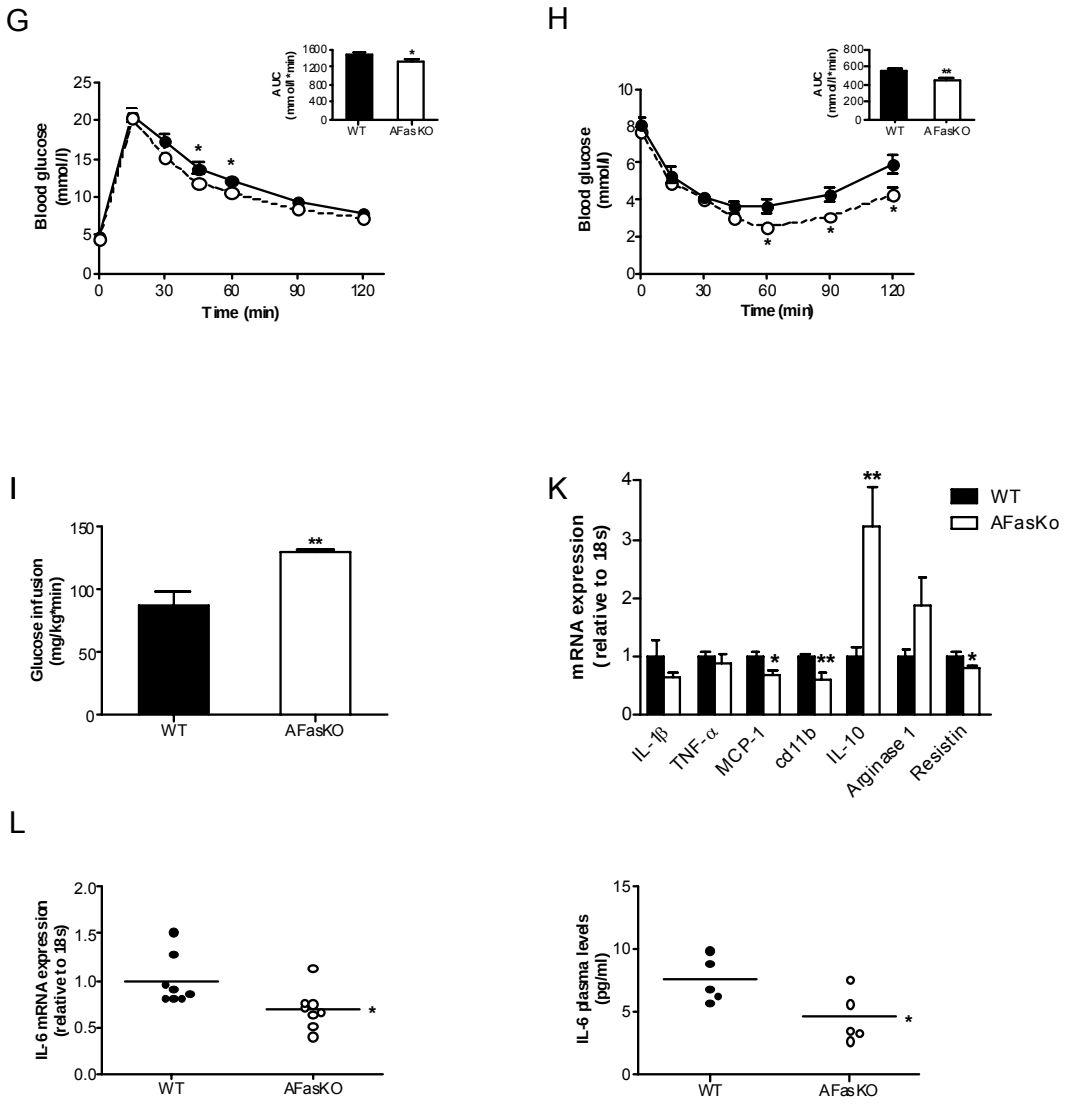

Fig. 3 **(A)** Total cell lysates were prepared from isolated adipocytes, resolved by LDS-PAGE and immunoblotted with anti-Fas or anti-actin antibody. **(B)** Total tissue lysates were resolved by LDS-PAGE and immunoblotted with anti-Fas or anti-actin antibody. **(C)** Total cell lysates (80 µg) from isolated adipocytes and macrophages were resolved by LDS-PAGE and immunoblotted with anti-Cre or anti-actin antibody. **(D)** Total cell lysates from activated and resident macrophages were resolved by LDS-PAGE and immunoblotted with anti-Fas or anti-actin antibody. **(E)** Size of isolated perigonadal adipocytes was determined. For each mouse, at least 100 adipocytes were analyzed. ImageJ software was used for quantification (National Institutes of Health, Bethesda, MD). The results represent the mean ± SEM of 4 to 5 different mice. **(F)** ^{14}C-D-glucose incorporation into isolated perigonadal adipocytes from WT (black bars) and AFasKO (white bars) mice was

determined in the absence or presence of insulin. Results are expressed relative to basal uptake and represent the mean ± SEM of 5 independent experiments performed in triplicates. *p < 0.05 (Student's *t* test). Intraperitoneal glucose (**G**) and insulin (**H**) tolerance tests were performed in wild-type (●) and AFasKO (○) mice. Inserted graphs in **G** and **H** depict the respective analysis of the area under the curve. Results are the means ± SEM of 8 to 10 animals per group. *p < 0.05, **p < 0.01 (Student's *t* test). (**I**) Steady-state glucose infusion rates during hyperinsulinemic-euglycemic clamps. Results are the means ± SEM of 3-4 animals per group. **p < 0.01 (Student's *t* test). (**K**) Quantitative RT-PCR detection of mRNA expression in adipose tissue. Results are the means ± SEM of 5-9 animals per group. *p < 0.05, **p < 0.01 (Student's *t* test). **(L)** Left panel: Quantitative RT-PCR detection of IL-6 mRNA expression. The level of mRNA expression was normalized to 18S RNA. Results represent the mean ± SEM of 8 animals per group. *p < 0.05 (Student's *t* test). Right panel: Plasma concentration of IL-6. Results represent the mean ± SEM of 5 animals per group. *p < 0.05 (Student's *t* test).

Blood glucose levels were significantly higher in WT mice after a 7-hour fasting period, whereas insulin and FFA levels did not differ between WT and AFasKO mice (table S2). Moreover, adipocytes isolated from AFasKO mice exhibited improved insulin-stimulated glucose incorporation (mainly reflecting lipogenesis, (*17*)), compared to adipocytes from WT mice after 6 weeks of HFD (fig. 3F). Further consistent with improved adipocyte insulin sensitivity in the absence of Fas expression in adipocytes, insulin still had a significant anti-lipolytic effect in isolated adipocytes of HFD-fed AFasKO mice, but not in adipocytes of WT mice (49±19% vs. 26±7%), whereas basal free fatty acid (FFA) release was not different between both groups. Thus, specific ablation of Fas expression in adipocytes was associated with protection against the metabolic effects of HFD-feeding in adipocytes, without affecting adipocyte size.

To examine if improved insulin responsiveness of adipocytes conferred by adipocyte-specific Fas-deletion had systemic consequences, glucose metabolism was assessed. There was no difference in glucose or insulin tolerance test between chow-fed 3-months-old AFasKO and wildtype littermates (data not shown). In contrast, following 6 weeks of HFD, AFasKO mice exhibited a mild but significantly improved glucose tolerance compared to Cre-negative littermates (fig. 3G). Moreover, AFasKO mice were significantly more insulin sensitive as assessed by insulin tolerance test (ITT) (fig. 3H). Finally, under hyperinsulinemic-euglycemic clamp, glucose infusion rate was significantly increased in AFasKO mice compared to WT littermates (fig. 3I), confirming improved whole-body insulin sensitivity. Jointly, we hereby

describe an adipocyte-specific Fas-KO mouse model, which is protected against adipocyte and whole-body insulin resistance induced by HFD-feeding.

Given that Fas may be involved in inflammatory processes, we next assessed its potential involvement in adipose tissue inflammation. mRNA levels of major inflammatory markers were assessed in adipose tissue of HFD-fed WT versus AFasKO mice. In the KO mice, fat mRNA-levels of IL-6 (fig. 3L), CD11b, MCP-1 and resistin were significantly decreased, whereas mRNA levels of the anti-inflammatory cytokine IL-10 and arginase 1 levels were increased (fig. 3K). Since adipose tissue is proposed to be a major source of circulating levels of cytokines such as MCP-1 and IL-6 (*18, 19*), we measured their levels in the circulation. Whereas circulating MCP-1 levels were not significantly different between WT and AFasKO mice after six weeks of HFD, IL-6 levels were ~40% lower in the KO mice (fig. 3L) and KC levels (murine IL-8 equivalent) tended to be decreased (table S2). Circulating levels of the adipokines resistin and leptin were not affected (table S2), the latter further consistent with a lack of significant effect of adipocyte-specific Fas deletion on whole-body fat mass. These results suggest that the pro-inflammatory profile of secreted products from adipose tissue of AFasKO mice in response to high fat feeding is diminished compared to WT mice.

The studies so far demonstrate that the absence of Fas in adipocytes alters cytokine expression in adipose tissue, reflecting either direct effect on adipocytes or a secondary effect on adipose tissue macrophages. To further assess these propositions, 3T3-L1 adipocytes were incubated with FasL for 12 hours. Such treatment increased the release of IL-6 and KC into the medium by 1.5±0.1-fold and 2.8±0.5, respectively ($p<0.05$ for both cytokines compared to unstimulated cells) (fig. S7). Moreover, macrophages adhered significantly more readily to FasL-treated 3T3-L1 adipocytes (25±9 % increase in an in-vitro macrophage-adipocyte adherence assay, $p<0.05$) (fig. S8). These findings correspond to the observation that AFasKO mice on HFD had decreased expression of adipose tissue CD11b (probably reflecting decreased infiltrating leukocytes) (fig. 3K), and collectively suggest a role for Fas as an activator of adipocyte-derived inflammation.

What is the mechanism for increased adipocyte Fas expression in obesity? Studies in 3T3-L1 adipocytes suggest that TNF-α and IL-1β, two key pro-inflammatory cytokines arising early in the inflammatory process, induce Fas expression (fig. S9). At later stages of adipose tissue inflammation, adipose tissue is infiltrated by inflammatory cells, such as T-cells and macrophages, which express and

secret FasL (*6*). Intriguingly, we found FasL mRNA to be up-regulated in WAT of obese and diabetic mice (fig. S10). Thus, it is very likely that the trigger to up-regulate Fas expression and activation in adipose tissue in obesity is the increased production of pro-inflammatory cytokines and FasL. Intriguingly, a similar regulation was previously shown for TNF, i.e. expression of TNF receptor was shown to be up-regulated by different cytokines as well as by TNF (*20, 21*). Thus, like many other inflammatory mediators that participate in feed-forward loops to enhance the inflammatory response, Fas appears to be both target and positive mediator of the pro-inflammatory cascade of adipose tissue in obesity.

Adipose tissue inflammation has been linked to hepatic manifestations of obesity. In particular, the degree of adipose tissue macrophage infiltration correlated to histo-pathological changes in the liver (*22*). Hence, we next addressed the possibility that by diminishing adipose tissue inflammation, adipocyte Fas deletion protects from hepatic insulin resistance and steatosis. Histological examinations and biochemical determination of total hepatic lipid content revealed that the livers of AFasKO mice were protected against liver steatosis induced by HFD (fig. 4A). Consistently, liver protein content of the lipid droplet protein ADRP and the lipogenic transcription factor PPARγ were decreased in AFasKO mice compared to WT (*23*) (fig. 4B). Moreover, mRNA levels of the fatty acid transporter CD36 were reduced by 27% ($p<0.05$) in livers of AFasKO mice (fig. S11). In addition, liver steatosis was associated with activation of the NF-κB signaling pathway (*24*). Intriguingly, activation of NF-κB was reduced by 35% in livers of AFasKO mice compared to wild-type mice, as assessed by phosphorylation of the p65 subunit of NF-κB (fig. S12).

Molecularly, liver resistance to insulin actions was suggested to be mediated by increased Ser307 phosphorylation on IRS1, and by increased expression of SOCS3 (*13*). Interestingly, AFasKO mice had 50% lower levels of IRS1 phosphorylation on Ser307 (fig. 4C). In addition, expression of SOCS3 mRNA levels (relative to 18S) was reduced by 25%. Circulating glucose levels following a pyruvate load suggested that AFasKO mice had lower gluconeogenic flux compared to wild-type mice on HFD (fig. 4D). Moreover, during a hyperinsulinemic-euglycemic clamp, insulin-induced suppression of hepatic glucose production was blunted in HFD-fed wild-type mice, but was clearly evident in AFasKO mice (fig. 4E). Although not experimentally tested herein, a possible candidate for mediating the hepatic steatosis/insulin resistance occurring in WT mice and diminished in AFasKO mice is IL-6. Indeed, IL-6 treatment of hepatocytes induced insulin resistance *in vitro (13, 25)* and it seems to be generally accepted that IL-6

causes hepatic insulin resistance (*18*). Particularly, IL-6 was shown to induce phosphorylation of IRS-1 on Ser307 residue and to activate the negative insulin signaling regulator SOCS3 in C57BL/6J mice (*26, 27*). Accordingly, IL-6 expression in adipose tissue and circulating IL-6 levels were reduced in HFD-fed AFasKO mice and their livers exhibited decreased Ser307-phosphorylation of IRS-1 and decreased mRNA levels of SOCS-3 compared to wild-type mice. Thus, overall, adipocyte-specific Fas-deletion diminishes adipose tissue inflammation and protects the liver from developing insulin resistance and hepatic steatosis.

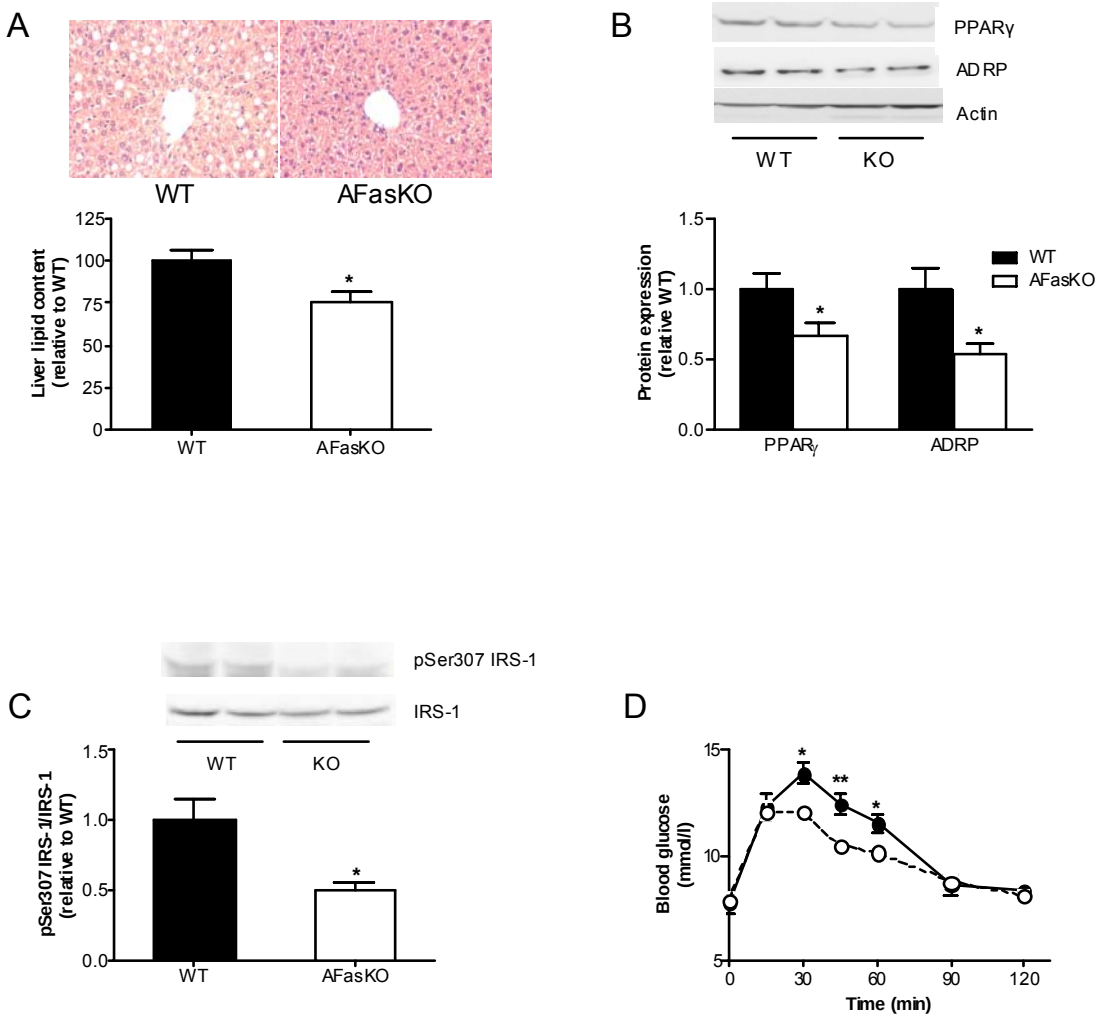

E

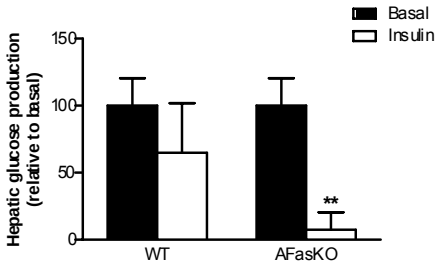

Fig. 4 **(A)** H&E stained liver sections from WT (left panel) and AFasKO (right panel) mice. Lower panel: Total liver lipids were determined and expressed relative to lipid content in wild-type mice. Results represent the mean ± SEM of 8 mice of each group. *p < 0.05 (Student's *t* test). **(B)** Liver lysates were resolved by LDS-PAGE and immunoblotted with ADRP, PPARγ or actin antibodies. A representative immunoblot is shown. Results are the means ± SEM of 4 to 6 animals per group and are expressed relative to protein expression in WT mice. *p < 0.05 (Student's *t* test). (**C**) Liver lysates were resolved by LDS-PAGE and immunoblotted with anti-phospho-IRS1 (Ser307) and total IRS-1 antibodies. Representative immunoblots are shown in the upper panel. Expression levels of pSer307 are normalized to expression of total IRS1. Results are the means ± SEM of 4 mice and are expressed relative to WT. *p < 0.05 (Student's *t* test). **(D)** Intraperitoneal pyruvate tolerance test was performed in wild-type (●) and AFasKO (○) mice. Results are the means ± SEM of 7 animals per group. *p < 0.05, **p < 0.01 (Student's *t* test). **(E)** Hepatic glucose production was calculated in the basal period and in response to insulin infusion during the hyperinsulinemic-euglycemic clamp study. Results are the means ± SEM of 3-4 animals per group and are expressed relative to basal hepatic glucose production. **p < 0.01 (Student's *t* test).

The relevance of our studies to human obesity are offered by our findings that Fas is up-regulated in adipose tissue of obese patients and even more so in obese diabetic patients (fig. 1C). This finding may hint towards a role of Fas in the development of obesity-induced insulin resistance in humans. Intriguingly, recent studies in humans revealed an association of promoter alterations in the Fas and FasL gene with type 2 diabetes and insulin resistance (*28*), further supporting such notion.

In conclusion, our findings suggest that Fas activation in adipocytes contributes to the increased production and secretion of inflammatory cytokines in obesity and, thus, contributes to the development of

hepatic and total body insulin resistance. Based on our findings, it would seem important to determine if inhibition of Fas expression/activation in adipocytes may constitute a potential new therapeutic target in the treatment of insulin resistance, type 2 diabetes, and fatty liver diseases.

Acknowledgement

This work was supported by grants from the Swiss National Science Foundation # 310000-112275 and a “Forschungskredit” from the University of Zurich (both to DK). We would like to greatly acknowledge Dr. Maggy Arras, for expert veterinary advice, and Prof. Kurt Bürki for advice regarding the breeding of lox and cre mice. We are indebted to Dr. Paolo Cinelli for his advice regarding mRNA preparation and determination.

All authors state no conflict of interest.

References

[1] Bashan N, Dorfman K, Tarnovscki T, et al. (2007) Mitogen-activated protein kinases, inhibitory-kappaB kinase, and insulin signaling in human omental versus subcutaneous adipose tissue in obesity. Endocrinology 148: 2955-2962

[2] Harman-Boehm I, Bluher M, Redel H, et al. (2007) Macrophage infiltration into omental versus subcutaneous fat across different populations: effect of regional adiposity and the comorbidities of obesity. J Clin Endocrinol Metab 92: 2240-2247

[3] Stranges PB, Watson J, Cooper CJ, et al. (2007) Elimination of antigen-presenting cells and autoreactive T cells by Fas contributes to prevention of autoimmunity. Immunity 26: 629-641

[4] Konrad D, Rudich A, Schoenle EJ (2007) Improved glucose tolerance in mice receiving intraperitoneal transplantation of normal fat tissue. Diabetologia 50: 833-839

[5] Rudich A, Konrad D, Török D, et al. (2003) Indinavir uncovers different contributions of GLUT4 and GLUT1 towards glucose uptake in muscle and fat cells and tissues. Diabetologia 46: 649-658

[6] Wueest S, Rapold RA, Rytka JM, Schoenle EJ, Konrad D (2008) Basal lipolysis, not the degree of insulin resistance, differentiates large from small isolated adipocytes in high-fat fed mice. Diabetologia: Epub ahead of print

[7] Knight JA, Anderson S, Rawle JM (1972) Chemical basis of the sulfo-phospho-vanillin reaction for estimating total serum lipids. Clin Chem 18: 199-202

[8] Pfaffl MW (2001) A new mathematical model for relative quantification in real-time RT-PCR. Nucleic Acids Res 29: e45

[9] Souza SC, Muliro KV, Liscum L, et al. (2002) Modulation of hormone-sensitive lipase and protein kinase A-mediated lipolysis by perilipin A in an adenoviral reconstituted system. J Biol Chem 277: 8267-8272

[10] Fukuzumi M, Shinomiya H, Shimizu Y, Ohishi K, Utsumi S (1996) Endotoxin-induced enhancement of glucose influx into murine peritoneal macrophages via GLUT1. Infect Immun 64: 108-112

[11] Wellen KE, Hotamisligil GS (2005) Inflammation, stress, and diabetes. J Clin Invest 115: 1111-1119

[12] Park SY, Cho YR, Kim HJ, et al. (2005) Unraveling the temporal pattern of diet-induced insulin resistance in individual organs and cardiac dysfunction in C57BL/6 mice. Diabetes 54: 3530-3540

[13] Zick Y (2005) Ser/Thr phosphorylation of IRS proteins: a molecular basis for insulin resistance. Sci STKE 2005: pe4

[14] Kanda H, Tateya S, Tamori Y, et al. (2006) MCP-1 contributes to macrophage infiltration into adipose tissue, insulin resistance, and hepatic steatosis in obesity. J Clin Invest 116: 1494-1505

[15] Xu H, Barnes GT, Yang Q, et al. (2003) Chronic inflammation in fat plays a crucial role in the development of obesity-related insulin resistance. J Clin Invest 112: 1821-1830

[16] Peter ME, Budd RC, Desbarats J, et al. (2007) The CD95 receptor: apoptosis revisited. Cell 129: 447-450

[17] Faouzi S, Burckhardt BE, Hanson JC, et al. (2001) Anti-Fas induces hepatic chemokines and promotes inflammation by an NF-kappa B-independent, caspase-3-dependent pathway. J Biol Chem 276: 49077-49082

[18] Farley SM, Purdy DE, Ryabinina OP, Schneider P, Magun BE, Iordanov MS (2008) Fas ligand-induced proinflammatory transcriptional responses in reconstructed human epidermis. Recruitment of the epidermal growth factor receptor and activation of MAP kinases. J Biol Chem 283: 919-928

[19] Imamura R, Konaka K, Matsumoto N, et al. (2004) Fas ligand induces cell-autonomous NF-kappaB activation and interleukin-8 production by a mechanism distinct from that of tumor necrosis factor-alpha. J Biol Chem 279: 46415-46423

[20] Miwa K, Asano M, Horai R, Iwakura Y, Nagata S, Suda T (1998) Caspase 1-independent IL-1beta release and inflammation induced by the apoptosis inducer Fas ligand. Nat Med 4: 1287-1292

[21] Schaub FJ, Liles WC, Ferri N, Sayson K, Seifert RA, Bowen-Pope DF (2003) Fas and Fas-associated death domain protein regulate monocyte chemoattractant protein-1 expression by human smooth muscle cells through caspase- and calpain-dependent release of interleukin-1alpha. Circ Res 93: 515-522

[22] Fischer-Posovszky P, Tornqvist H, Debatin KM, Wabitsch M (2004) Inhibition of death-receptor mediated apoptosis in human adipocytes by the insulin-like growth factor I (IGF-I)/IGF-I receptor autocrine circuit. Endocrinology 145: 1849-1859

[23] Sabio G, Das M, Mora A, et al. (2008) A stress signaling pathway in adipose tissue regulates hepatic insulin resistance. Science 322: 1539-1543

[24] Pisetsky DS, Caster SA, Roths JB, Murphy ED (1982) Ipr gene control of the anti-DNA antibody response. J Immunol 128: 2322-2325
[25] Makowski L, Boord JB, Maeda K, et al. (2001) Lack of macrophage fatty-acid-binding protein aP2 protects mice deficient in apolipoprotein E against atherosclerosis. Nat Med 7: 699-705
[26] He W, Barak Y, Hevener A, et al. (2003) Adipose-specific peroxisome proliferator-activated receptor gamma knockout causes insulin resistance in fat and liver but not in muscle. Proc Natl Acad Sci U S A 100: 15712-15717
[27] Wueest SM, Rapold RA, Rytka JM, Schoenle EJ, Konrad D (2008) Basal biolysis, not the degree of insulin resistance, differentiates large from small isolated adipocytes in high-fat fed mice. Diabetologia epub ahead
[28] Carey AL, Febbraio MA (2004) Interleukin-6 and insulin sensitivity: friend or foe? Diabetologia 47: 1135-1142
[29] Sartipy P, Loskutoff DJ (2003) Monocyte chemoattractant protein 1 in obesity and insulin resistance. Proc Natl Acad Sci U S A 100: 7265-7270
[30] Bradley JR (2008) TNF-mediated inflammatory disease. J Pathol 214: 149-160
[31] Winzen R, Wallach D, Kemper O, Resch K, Holtmann H (1993) Selective up-regulation of the 75-kDa tumor necrosis factor (TNF) receptor and its mRNA by TNF and IL-1. J Immunol 150: 4346-4353
[32] Cancello R, Tordjman J, Poitou C, et al. (2006) Increased infiltration of macrophages in omental adipose tissue is associated with marked hepatic lesions in morbid human obesity. Diabetes 55: 1554-1561
[33] Inoue M, Ohtake T, Motomura W, et al. (2005) Increased expression of PPARgamma in high fat diet-induced liver steatosis in mice. Biochem Biophys Res Commun 336: 215-222
[34] Cai D, Yuan M, Frantz DF, et al. (2005) Local and systemic insulin resistance resulting from hepatic activation of IKK-beta and NF-kappaB. Nat Med 11: 183-190
[35] Senn JJ, Klover PJ, Nowak IA, Mooney RA (2002) Interleukin-6 induces cellular insulin resistance in hepatocytes. Diabetes 51: 3391-3399
[36] Senn JJ, Klover PJ, Nowak IA, et al. (2003) Suppressor of cytokine signaling-3 (SOCS-3), a potential mediator of interleukin-6-dependent insulin resistance in hepatocytes. J Biol Chem 278: 13740-13746
[37] Weigert C, Hennige AM, Lehmann R, et al. (2006) Direct cross-talk of interleukin-6 and insulin signal transduction via insulin receptor substrate-1 in skeletal muscle cells. J Biol Chem 281: 7060-7067
[38] Nolsoe RL, Hamid YH, Pociot F, et al. (2006) Association of a microsatellite in FASL to type II diabetes and of the FAS-670G>A genotype to insulin resistance. Genes Immun 7: 316-321

Supplemental Figures and Tables

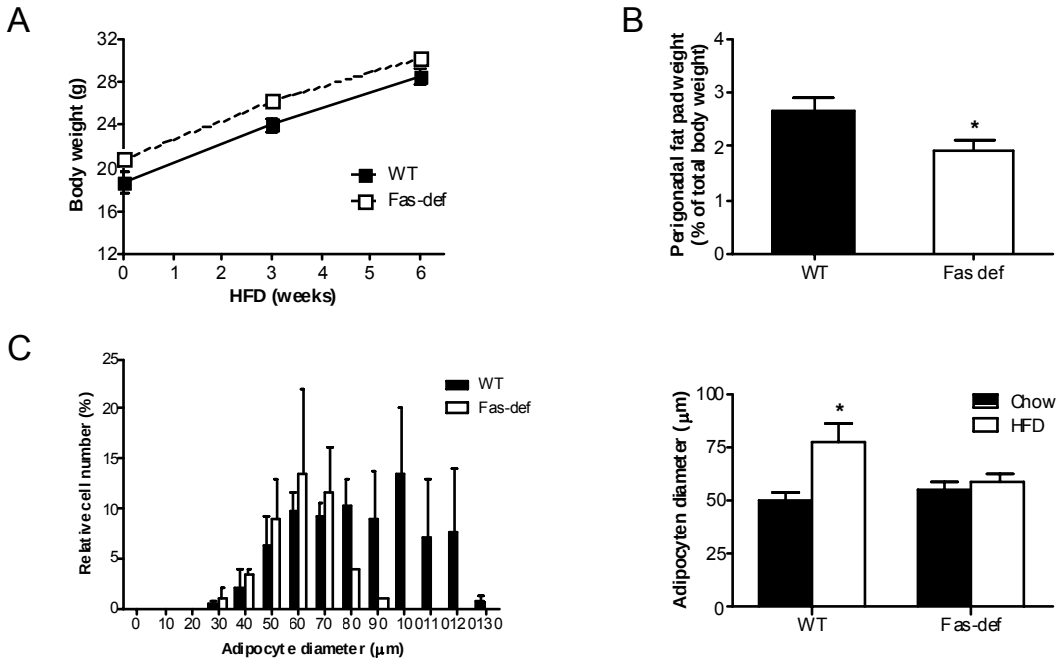

Fig. S1 Reduced fat pad weight and adipocyte size in HFD-fed Fas-def mice
(A) Weight gain was analyzed in HFD-fed WT (■) and Fas-def (□) mice. Results are the means ± SEM of 14 to 15 animals per group. **(B)** Perigonadal fat pad weight (expressed as fat pad weight per body weight) was analyzed. Results are the means ± SEM of 10 to 15 animals per group. *$p < 0.05$ (Student's *t* test). **(C)** Left panel: Relative size distribution of adipocyte diameter after 6 weeks of HFD in WT and Fas-def mice was analyzed. Results represent the mean ± SEM of 3-4 independent experiments. Right panel: Mean adipocyte diameter of chow- and HFD-fed Fas-def and WT mice is depicted. Results represent the mean ± SEM of 3 independent experiments. *$p < 0.05$ (Student's *t* test).

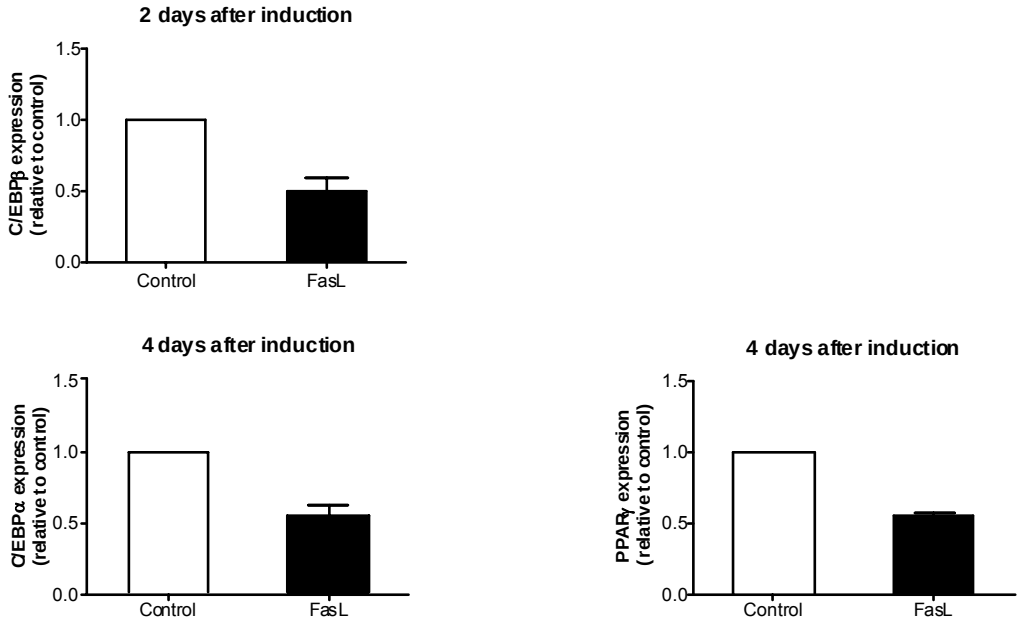

Fig. S2 FasL treatment decreases expression of adipocyte differentiation markers
After reaching confluence, 3T3-L1 praeadipocytes were incubated with or without 2ng/ml FasL. Differentiation was induced 48 hours later with isobutylmethylxanthine (IBMX), dexamethasone, insulin and rosiglitazone. Total cell lysates were resolved by LDS-PAGE and immunoblotted with anti-C/EBPß, anti-C/EBPa or anti-PPAR? antibody. Results are the means ± SEM of 2-3 independent experiments.

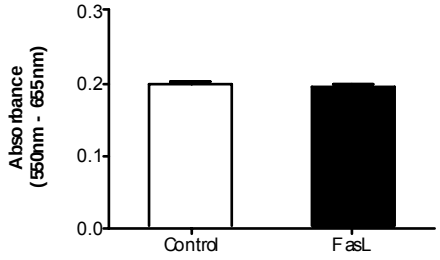

Fig. S3 Fas-ligation for 12 hours does not affect viability of 3T3-L1 adipocytes
Mature 3T3-L1 adipocytes were incubated for 12 hours with 2ng/ml FasL. Thereafter, cells were incubated with MTT. Salt was extracted from the cells with DMSO. The amount of yellow MTT reduced to purple formazan was measured spectrophotometrically. Results are the mean ± SEM of 3 independent experiments.

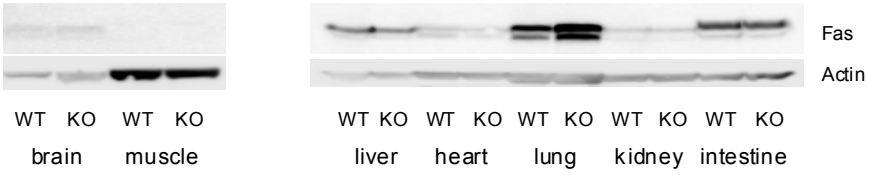

Fig. S4 Fas expression in different tissues harvested from WT and AFasKO mice
Total tissue lysates were prepared and resolved by LDS-PAGE and immunoblotted with anti-Fas or anti-actin antibody.

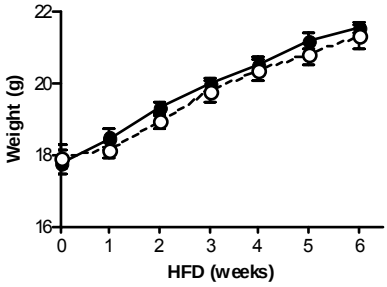

Fig. S5 Similar weight gain in WT and AFasKO mice after six weeks of high fat diet
Weight gain was analyzed in wild-type (●) and AFasKO (○) mice. Results are the means ± SEM of 14 to 15 animals per group.

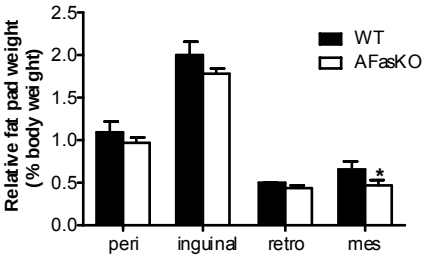

Fig. S6 Similar fat pad weight in WT and AFasKO mice after six weeks of high fat diet
Different fat pads were harvested and weighted. Results are expressed relative to total body weight and represent the mean ± SEM of 14 mice group. *p < 0.05 (Student's *t* test). Peri: perigonadal; retro: retroperitoneal; mes: mesenteric.

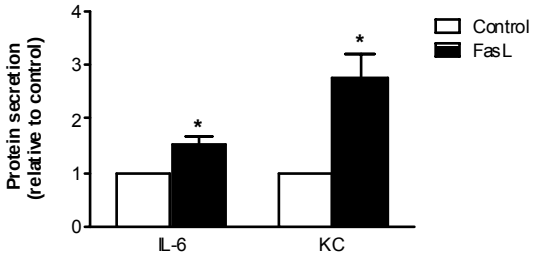

Fig. S7 Fas-ligation increases expression of pro-inflammatory cytokines in 3T3-L1 adipocytes
Mature 3T3-L1 adipocytes were incubated in the presence (black bars) or absence (white bars) of 2ng/ml FasL for 12 hours. Medium was removed and cells were incubated with KREBS buffer. Cytokines were then determined in the supernatant. Shown are results normalized to untreated cells. Results represent the mean ± SEM of 4 to 5 independent experiments. *p < 0.05 (One sample *t* test).

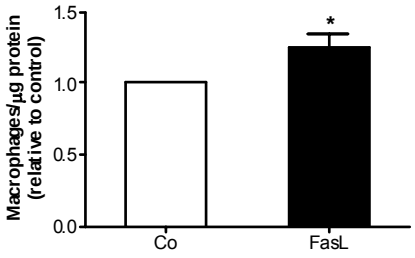

Fig. S8 Macrophage adherence is increased in FasL-treated 3T3-L1 adipocytes
Mature 3T3-L1 adipocytes were incubated in the presence (black bars) or absence (white bars) of 2ng/ml FasL for 12 hours. Thereafter adipocytes were incubated with ^{3}H-labeled macrophages for one hour at 37°C. Cells were washed and lysed (0.05N NaOH). Finally, radioactivity of lysates was determined by a ß-counter. Results represent the mean ± SEM of 7 independent experiments. *p < 0.05 (One sample *t* test).

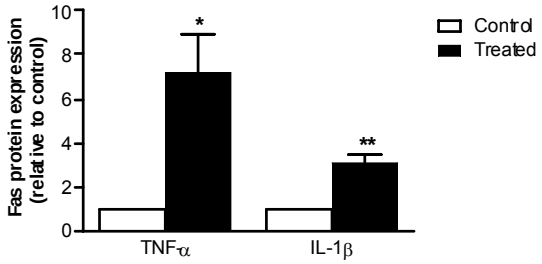

Fig. S9 Fas expression is induced by pro-inflammatory cytokines in 3T3-L1 adipocytes
Mature 3T3-L1 adipocytes were incubated with 5nM TNF-a or 20 ng/ml IL-1ß for 12 hours. Total cell lysates were resolved by LDS-PAGE and immunoblotted with anti-Fas antibody. Results are the means ± SEM of 4 independent experiments and are expressed relative to untreated cells. *p < 0.05, **p < 0.01 (One sample *t* test).

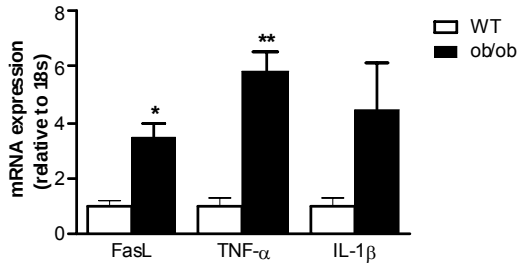

Fig. S10 Increased FasL expression *ob/ob*-mice
Total RNA was extracted from perigonadal fat pads and quantitative RT-PCR was performed. The level of mRNA expression was normalized to 18S RNA. Results represent the mean ± SEM of 3 animals per group. *p<0.05; **p<0.01 (Student's t test).

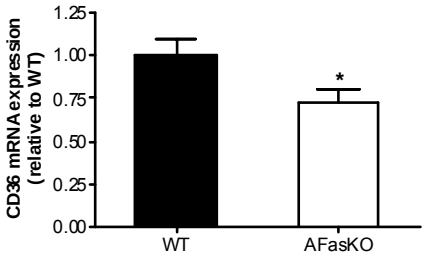

Fig. S11 Hepatic CD36 mRNA levels are significantly decreased in AFasKO mice
mRNA expression of CD36 in liver tissues of wildtype and AFasKO mice was analyzed. Results are the means ± SEM of 9 mice of each group, expressed relative to WT and normalized to expression of 18S. *p < 0.05 (Student's t test).

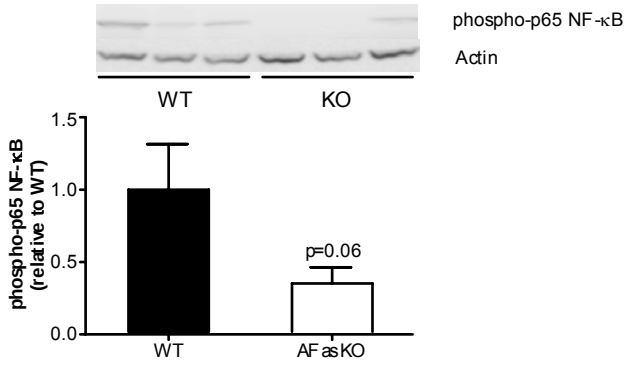

Fig. S12 phospho-p65 is reduced in livers of AFasKO mice
Liver lysates were prepared from WT and AFasKO mice and resolved by LDS-PAGE. Lysates were immunoblotted with anti-phospho-p65 NF-kB or anti-actin antibodies. Representative immunoblots are shown in the upper panel. Expression levels of phospho-p65 are normalized to expression of actin. Results are the means ± SEM of 5 to 6 mice and are expressed relative to WT.

Table S1 Basic clinical characteristics of patients

	Lean (n=3)	*Obese (n=3)*	*Obese and diabetic (n=3)*
Age (y)	44.0±2.5	29.7±10.0	48.3±2.7
BMI (Kg/m2)	23.6±1.0	44.3±1.4	42.1±0.8
FPG (mg/dl)	87±4	85±4	197±80
Fasting insulin	8.9±2.7	18.5±5.2	7.3±4.5
HbA1C (%)	5.4±0.2	5.8±0.2	7.9±1.4
Triglycerides (mg/dl)	89±4	110±9	204±43
Total cholesterol (mg/dl)	182±6	185±18	256±27

Table S2 Plasma levels of glucose, insulin, adipokines and cytokines of HFD-fed wild-type (WT) and AFasKO mice

	WT	AFasKO
Blood glucose	10.6 ± 0.3	9.4 ± 0.4 *****
Insulin (pmol/l)	98.5 ± 17.7	89.1 ± 7.8
Resistin (pg/ml)	4465 ± 516	5251 ± 730
Leptin (pg/ml)	1270 ± 305	1240 ± 209
MCP-1 (pg/ml)	47.5 ± 12.9	35.1 ± 7.8
IL-6 (pg/ml)	7.6 ± 0.9	4.6 ± 1.0 *****
KC (pg/ml)	481 ± 139	278 ± 54
TNF-α	n.d.	n.d.

Results are the means ± SEM of five to nine independent experiments. *p < 0.05 (Student's *t* test). n.d. not detectable